Catalysis Letters Vol. 103, Nos. 1–2, September 2005 (© 2005)
DOI: 10.1007/s10562-005-6510-x

Hydroisomerization of long-chain alkane over Pt/SAPO-11 catalysts synthesized from nonaqueous media

Zheming Wang[a], Zhijian Tian[a,*], Fei Teng[a], Guodong Wen[a], Yunpeng Xu[a], Zhusheng Xu[a], and Liwu Lin[a,b]

[a]*Laboratory of Natural Gas Utilization and Applied Catalysis, Dalian Institute of Chemical Physics, Chinese Academy of Sciences, 457, Zhongshan Road Dalian, 116023, P. R. China*

[b]*State Key Laboratory of Catalysis, Dalian Institute of Chemical Physics, Chinese Academy of Sciences, 457 Zhongshan Road, Dalian, 116023 P. R. China*

Received 2 May 2005; accepted 4 May 2005

SAPO-11 molecular sieves were synthesized from nonaqueous media. The effects of Si and Al sources as well as solvents on the catalytic performance of SAPO-11 were investigated by the hydroisomerization reaction of *n*-dodecane. The samples were characterized by XRD, XRF, N_2-adsorption, SEM, NH_3-TPD, IR-NH_3 and ^{29}Si CP MAS NMR. The SAPO-11 samples synthesized with tetraethoxysilane as the Si source showed higher Si incorporation contents than the SAPO molecular sieves prepared with polymeric Si sources (fumed silica and Si colloidal gel). The reaction results showed that Pt/SAPO-11 catalysts synthesized from ethylene glycol and glycerol media with the monomeric Si and Al sources (tetraethoxysilane, aluminum isopropoxide) exhibited higher catalytic activities than those catalysts with the polymeric Si or Al (pseudo-boehmite) sources, due to the larger external surface area and higher acidity of the former ones. Especially, the catalyst synthesized in an ethylene glycol medium possessed the highest catalytic activity. Over this catalyst, 88% conversion of *n*-dodecane was achieved at a low temperature of 250 °C.

KEY WORDS: Nonaqueous synthesis; Si sources; Al sources; solvents; SAPO-11; hydroisomerization; *n*-Dodecane.

1. Introduction

Hydroisomerization of long chain alkanes is of great significance in petrorefining and petrochemical industries for producing high viscosity index lube oils with low pour points [1,2]. Hydroisomerization reactions are usually carried out over bi-functional catalysts having metal sites for the hydrogenation-dehydrogenation and acidic sites for C–C skeleton rearrangements. If the hydrogenation ability is high enough, then the hydroisomerization selectivity of the bi-functional catalysts is mainly dependent on the pore structure [3–5] and the acidity [6–8]. Some research works [7,8] have revealed that decreasing of the catalyst acidity is beneficial for reducing the cracking activity. It was showed that medium-pored ZSM-22 [5,9], ZSM-23 [10] and SAPO-11 [2–4, 11–13] molecular sieves loaded with Pt or Pd exhibited high hydroisomerization selectivities. Over these molecular sieve catalysts having mono-dimensional 10-membered ring pore channels, multi-branched isomers which are susceptible to cracking could be suppressed, thus leading to a high isomerization selectivity. For bi-functional catalysts, acidity is one of the key factors in determining the catalytic activities of the catalysts [14,15]. Since SAPO-11 only possesses mild acidity [16], so Pt/SAPO-11 catalysts will exhibit lower activities than the aluminosilicate zeolite catalysts. Thus, it is desirable to increase the number of acid sites as well as the acidic strength of SAPO-11 so as to improve the catalytic activity of its supported catalysts.

The acidity of the SAPO molecular sieves depends strongly on the Si content and the mechanism of Si substitution [15–18]. When Si atoms are introduced to the phosphorous sites of a theoretical $AlPO_4$ framework (SM2 substitution), Bronsted acid sites will be formed [16]. On the contrary, simultaneous replacement of a pair of Al and P atoms by two Si atoms (SM3 substitution) will lead to a neutral framework. In addition, the Bronsted acid sites can also be generated by a combination of the SM3 substitution with the SM2 substitution [18]. The resulting acidic strength is usually stronger than that arising by a simple SM2 substitution [19,20]. It was shown [13,21] that acidic sites locating at the border of "Si islands" formed by a SM2 + SM3 substitution possess high catalytic activities for the hydroconversion of alkanes.

Normally, $AlPO_4$-*n* and SAPO molecular sieves are synthesized from an aqueous medium. Xu and Sinha et al. have developed a nonaqueous route for the synthesis of $AlPO_4$-*n* [22,23] and SAPO molecular sieves [12,24,25]. It was found that nonaqueous media favored Si incorporation and altered the Si dispersion in the framework of the SAPO molecular sieves[24,25]. In this work, we report on the synthesis of SAPO-11 molecular sieves from both aqueous and nonaqueous media by

* To whom correspondence should be addressed.
E-mail: tianz@dicp.ac.cn

using different Si sources, Al sources and solvents. Then physico-chemical properties of all the samples were compared. *n*-Dodecane was used as a model reactant of long chain alkane to investigate the catalytic activity of Pt/SAPO-11 catalysts which were prepared by supporting Pt on the SAPO-11 molecular sieves prepared in nonaqueous media. It was found that the catalysts supported on the SAPO-11 prepared from nonaqueous media using monomeric Si and Al sources (tetraethoxysilane and aluminum isopropoxide, respectively) exhibited excellent hydroisomerization performances.

2. Experimental

2.1. Preparation of catalysts

The reagents used in the synthesis were aluminum isopropoxide (IPA:AR), pseudo-boehmite (PB: 78.4Al_2O_3%), Si colloidal gel (SS: 30SiO_2%), fumed silica (FS: 99SiO_2%) , tetraethoxysilane (TEOS, AR), phosphoric acid (85%) and di-*n*-propylamine (DPA, AR). Ethylene glycol (EG, AR) and glycerol (AR) were used as nonaqueous solvents. All the reagents were purchased from Shanghai Med. Chem. Co (China) and used without further purification.

In a typical procedure for the synthesis of SAPO-11 from a nonaqueous medium, IPA was first mixed with DPA and EG, and stirred for 2 h. Then, phosphoric acid was added to the mixture, and stirred for another 2 h. Finally, TEOS was added to this mixture, and stirred continuously for 2 h. The molar composition of the synthesis gel was 0.2 SiO_2:1.0 Al_2O_3:1.8P_2O_5: 5.0DPA:55.0EG. The final mixture was transferred into a stainless-steel autoclave and was heated at 200 °C for 8 days. For comparison, SAPO-11 was also hydrothermally synthesized from an aqueous medium with tetraethoxysilane and aluminum isopropoxide as the Si and Al sources at 200 °C for 2 days, with a similar procedure mentioned above. The chemical molar composition of the synthesis gel was 0.2 SiO_2:1.0Al_2O_3:1.0P_2O_5: 1.0DPA:55.0H_2O.

The as-synthesized products were washed, dried at 393 K for 12 h and then calcinated at 873 K for 24 h in order to remove the organic templates completely. All the catalysts with 0.5 wt% Pt were prepared by a wetness impregnation method using a $Pt(NH_3)_4{\cdot}Cl_2$ solution.

2.2. Catalyst characterization

X-ray powder diffraction (XRD) patterns were recorded by a Philips CX' Pert PRO diffractometer using CuK_α radiation ($\lambda = 1.5404$) and Ni filter, operating at 40 kV, 40 mA and 2θ scanning speed of 5° min^{-1}. The relative crystallinities of the samples were calculated by summing up the areas of the peaks in the 2θ range from 20 to 23°. X-rays fluorescence (XRF) analysis was performed on a Philips Magix X X-ray fluorescence apparatus. Surface areas and pore distributions were determined on a Micromeritics ASAP 2010 physical analyzer by N_2 adsorption (77 K). Microporous distributions were determined by the HK method, and the external surface areas of the samples were calculated by the *t*-plot method. The morphology of the products was examined by a JEOL JSN-6460LV scanning electron microscope (SEM). The acidic amounts of the samples were determined by pulse adsorption of NH_3. Prior to the adsorption of NH_3, the samples were pretreated *in situ* in flowing He at 773 K for 1 h and saturated with pulsed NH_3 at 373 K. NH_3-TPD measurements were carried out from 373 K to 873 K, with a heating rate of 10 K min^{-1}. IR spectra of desorbed NH_3 were recorded on a Bruker EQUINOX 55 spectrometer at a scanning range of 400 to 4000 cm^{-1}. Self-supporting IR wafers of about 10 mg/cm^2 were first evacuated *in situ* at 773 K for 1 h, then the spectra were recorded after cooling to room temperature. NH_3 was admitted, and after equilibrium the samples were degassed at 373, 473 and 573 K, respectively, and the corresponding spectra were recorded. ^{29}Si solid NMR spectra were measured at room temperature on a Varian Infinityplus-400 spectrometer using 7.5 mm ZrO_2 rotors. ^{29}Si CP/MAS NMR spectra were recorded at 79.5 MHZ using 2.8 μs pulse, 3 s delay time, 3.0 ms contact time, and 4092 scans. All ^{29}Si spectra were recorded on samples spun at 4 KHz and referenced to DSS.

2.3. Catalytic evaluation

Prior to the reaction, the catalysts were reduced in flowing hydrogen at 723 K for 2 h. Hydroisomerization of *n*-dodecane (*n*-C_{12}) was carried out in a fixed-bed continuous reactor at atmospheric pressure. The reaction conditions were H_2/*n*-C_{12} (mol/mol) = 15, weight hourly space velocity (WHSV) = 1.0 h^{-1}, and reaction temperature ranging from 473 K to 673 K. The reactant and the products were analyzed on-line by a gas chromatograph (Varian Co. CP3800), equipped with a flame ionization detector and an OV-101 capillary column.

3. Results and discussion

3.1. Structures and chemical compositions

The starting materials, chemical compositions and crystallinities of all the samples synthesized from both aqueous and nonaqueous media are presented in table 1. The sample synthesized from an aqueous medium, with TEOS and IPA as the Si and Al sources, respectively, was denoted as S0. The samples synthesized from nonaqueous media with different Si sources, Al sources and solvents were denoted as S1∼S5.

The X-ray powder diffraction patterns identified that all the samples synthesized from both aqueous and nonaqueous media all possessed the AEL structure (as

Table 1
Starting materials, chemical composition and crystallinities of the SAPO-11 samples

Samples	Starting materials	Product compositions[c](mol)	Relative crystallinities(/%)
S0(aqu[a])	TEOS, IPA, H_2O	$Si_{0.012}Al_{0.563}P_{0.425}O_2$	85
S1(nonaqu[b])	Si colloidal gel, IPA,EG	$Si_{0.016}Al_{0.485}P_{0.499}O_2$	97
S2(nonaqu)	Fumed silica, IPA, EG	$Si_{0.023}Al_{0.481}P_{0.496}O_2$	80
S3(nonaqu)	TEOS, IPA, EG	$Si_{0.041}Al_{0.475}P_{0.484}O_2$	65
S4(nonaqu)	TEOS, SB, EG	$Si_{0.038}Al_{0.481}P_{0.481}O_2$	100
S5(nonaqu)	TEOS, IPA, glycerol	$Si_{0.044}Al_{0.477}P_{0.479}O_2$	75

[a]synthesized from an aqueous medium; [b]synthesized from nonaqueous media; [c]determined by XRF.

shown in figure 1). These samples exhibited a low background and no additional peaks were observed, which indicated that these samples were free from phase impurities. The relative crystallinities of all the samples decreased in the order: S4(100%) > S1(97%) > S0(85%) > S2(80%) > S5(75%) > S3(65%). In addition, it was observed that the XRD line of the S3 sample synthesized from a nonaqueous medium, with EG as the solvent, TEOS and IPA as the Si and Al sources, respectively, became broader compared with the other samples, indicating that the S3 sample had a smaller crystal size.

Comparing with the S0 sample synthesized from an aqueous medium, all the samples synthesized from nonaqueous media showed higher Si contents, which is in an agreement with Sinha's results [24,25]. It was proposed that the slow delivery of Si from the gel phase to the growing crystalline phase in a nonaqueous medium is beneficial for incorporating more Si atoms into the framework of SAPO-11. By comparing the Si contents of the samples synthesized from nonaqueous media, it can be found that the incorporation content of Si is strongly dependent on the types of the Si sources. The S3, S4 and S5 samples synthesized from nonaqueous media using a monomeric Si source (TEOS) possessed higher Si contents, as compared with the other samples prepared with polymeric Si sources (fumed silica or Si colloidal gel). As a monomeric Si source, TEOS might release active silicate intermediates by hydrolyzing faster in nonaqueous media than the polymeric Si sources (fumed silica or Si colloidal gel), and this can promote more Si to be incorporated into the structure of the SAPO-11 molecular sieves.

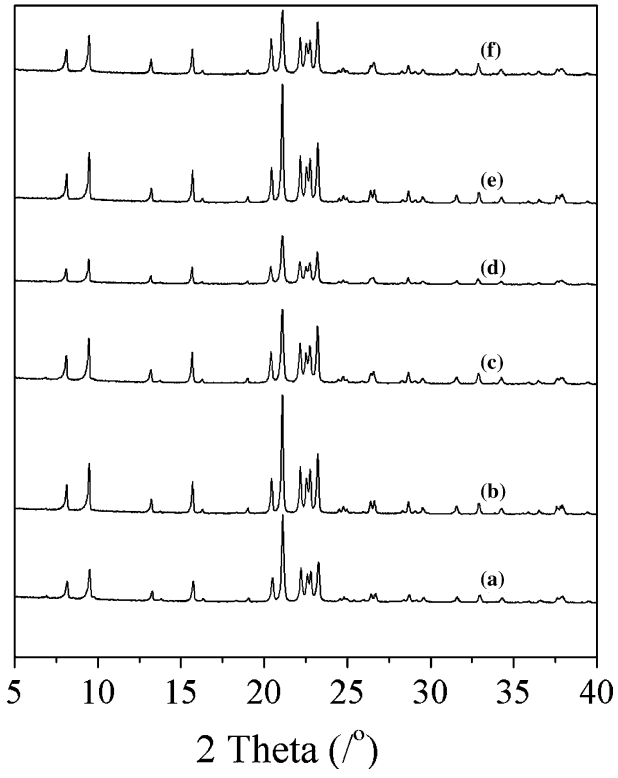

Figure 1. XRD patterns of the SAPO-11 samples [(a) S0 (TEOS, IPA, H_2O); (b) S1 (Si colloidal gel, IPA, EG); (c) S2 (Fumed silica, IPA, EG); (d) S3(TEOS, IPA, EG); (e) S4(TEOS, PB, EG); (f) S5(TEOS, IPA, glycerol)].

3.2. Surface area and surface morphology

The specific surface area (BET), microporous surface area and external surface area of the samples are listed in table 2. The SAPO-11 samples synthesized from nonaqueous media had not only larger BET surface areas, but also had larger external surface areas than that of the S0 sample synthesized from the aqueous medium. Among all the samples, the S3 and S5 samples synthesized from EG and glycerol media, respectively, had a relatively larger external surface area.

Scanning electron micrographs of the samples are shown in figure 2. The S0 sample synthesized from an aqueous medium exhibited irregular surface morphology, which consisted of cubic crystallites with a size of 2–4 μm. Due to different starting materials, the surface morphology and crystallite size of the samples synthesized from the nonaqueous media were also different. The S1 sample was composed of irregular blocks, with a size of about 3–5 μm. The S4 sample was comprised of plates, with a size of about 5 μm. Among all the samples, the S2, S3 and S5 samples had smaller crystallite sizes, which is in an agreement with the results of N_2-adsorption. The S5 sample was comprised by elliptic plates of 3–5 μm, with a thickness of only about 0.1 μm. The S2 sample consisted of crystallites with the size of 1×0.2 μm. For all the samples, the S3 sample synthesized from the nonaqueous EG medium and with TEOS and IPA as the Si and Al sources, respectively, had the smallest crystallite size, and consisted of rod-like crystallites with a diameter of about 0.1 μm.

3.3. Acidity and ^{29}Si CP/MAS NMR characterization

The NH_3-TPD patterns of the samples are shown in figure 3. The NH_3-TPD profiles display two peaks for all the samples. The low temperature peak around 180–200 °C corresponds to the desorption of NH_3 from the weak acidic sites, whilst the high temperature peak around 270–290 °C to that from the strong acidic sites. The weak acidic sites might be given rise by terminal P–OH groups [26], and the strong acidic sites are attributed to the bridging SiOHAl groups [27]. Table 2 gives the acidities of the samples synthesized from both aqueous and nonaqueous media. The number of strong acidic sites of all the samples decreased in the sequence of S3 > S5 > S2 > S4 > S1 > S0. The samples synthesized from nonaqueous media had more strong acidic sites than the S0 sample synthesized from the aqueous medium. Due to different starting materials, the acidities of the samples synthesized from nonaqueous media were not the same. The S3 and S5 samples synthesized from EG and glycerol media, respectively, with TEOS as the Si source and IPA as the Al source, had higher acidities, as compared with the samples synthesized with polymeric Si or Al sources. Especially, the S3 sample synthesized from the EG medium showed the highest acidity.

The number of strong acid sites per Si atom for all the samples decreased in the order of, S0 (0.82) > S1 (0.72) > S2 (0.63) > S3 (0.42) > S5 (0.36) > S4 (0.33), (see table 2). This fact can be interpreted in terms of the increasing likelihood of SM3 + SM2 substitution for the samples synthesized from the nonaqueous media [18]. For SAPO molecular sieves, simple SM2 substitution will lead to the formation of one Bronsted acid site per

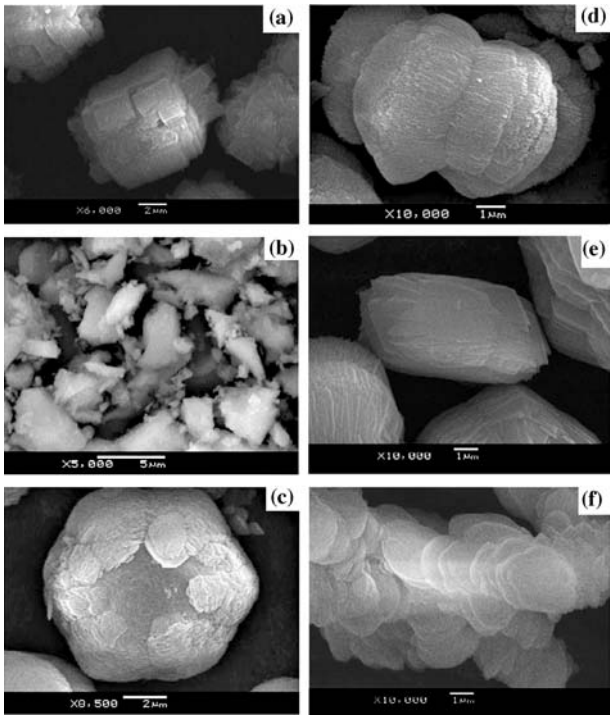

Figure 2. Surface morphology of the SAPO-11 samples [(a) S0 (TEOS, IPA, H_2O); (b) S1 (Si colloidal gel, IPA, EG); (c) S2 (Fumed silica, IPA, EG); (d) S3 (TEOS, IPA, EG); (e) S4(TEOS, PB, EG); (f) S5(TEOS, IPA, glycerol)].

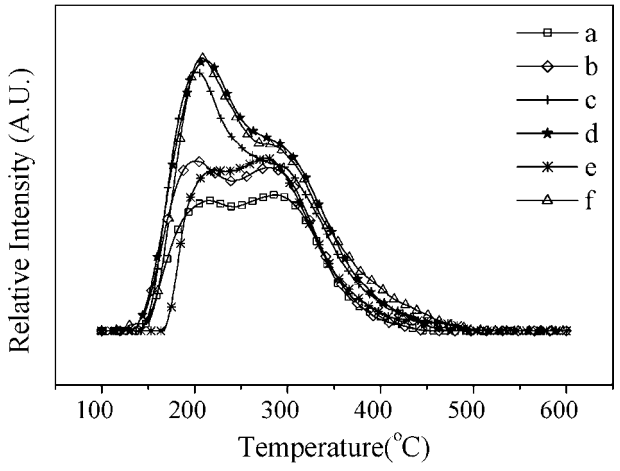

Figure 3. NH_3-TPD patterns of the SAPO-11 samples [(a) S0 (TEOS, IPA, H_2O); (b) S1(Si colloidal gel, IPA,EG); (c) S2 (Fumed silica, IPA, EG); (d) S3 (TEOS, IPA, EG); (e) S4(TEOS, PB, EG); (f) S5(TEOS, IPA, glycerol)].

Table 2
Surface area and acidic distribution of the SAPO-11 samples

Samples	Surface area/$m^2\ g^{-1}$			Acidic amount/mmol g^{-1}		Strong acid site/Si atom[e]
	S_{total}[a]	S_{micro}[b]	S_{ex}[c]	Strong[d]	total	
S0 (TEOS, IPA, H_2O)	173.0	165.7	7.3	0.162	0.217	0.82
S1 (Si colloidal gel, IPA, EG)	212.5	193.2	19.3	0.194	0.265	0.72
S2 (Fumed silica, IPA, EG)	227.3	196.1	31.2	0.236	0.344	0.63
S3 (TEOS, IPA, EG)	208.5	165.7	42.8	0.272	0.371	0.42
S4 (TEOS, PB, EG)	183.3	168.7	14.5	0.203	0.271	0.33
S5 (TEOS, IPA, glycerol)	234.9	194.1	40.9	0.255	0.377	0.36

[a]total surface area; [b]external surface area; [c]microporous surface area; [d]the strong acidic sites, NH_3-desorbed peak temperature about 270∼280 °C; [e]the number of strong acid sites per Si atoms.

Si atom, while SM3 + SM2 substitution will result in less than one acid site per Si atom [16,17]. Accordingly, for the S0 sample synthesized from an aqueous medium, the number of acidic sites per Si atoms was close to 1, implying that most of the Si atoms might be incorporated into the framework in the mode of isolated SM2 substitution. In contrast, the decrease of the number of acid sites per Si atom for the samples synthesized from nonaqueous media means that much more Si atoms were probably incorporated into the framework of these samples via SM2 + SM3 substitution. Furthermore, it was found that although the Si contents of the S3, S4 and S5 samples synthesized from nonaqueous media were very close (table 1), the acidity of the S4 sample was lower than those of the S3 and S5 samples. According to the model of Barthomeuf et al. [28], as the size of Si islands increases, the number of acidic sites of the SAPO zeolites will decrease. Therefore, the lower acidity of the S4 sample can be attributed to the formation of large Si islands in the framework.

Due to the low Si content of SAPO-11, ^{29}Si MAS NMR measurements of the SAPO-11 samples were unsuccessful. So $^1H \rightarrow {}^{29}Si$ CP/MAS NMR measurements were performed to give some information on the chemical environment of Si in the framework of the SAPO-11 samples. As shown in figure 4, the ^{29}Si CP/MAS NMR spectrum for the S0 sample synthesized from an aqueous medium displays only two peaks, and the peaks at −90 ppm and −95 ppm might be due to Si(4Al) and Si(3Al) species, respectively[13,21]. Comparing with the S0 sample synthesized from the aqueous media, the S3 and S4 samples synthesized from nonaqueous media exhibited much broader NMR lines in the range of −75 to −120 ppm. This indicates that, besides the Si(4Al) and S(3Al) coordination environments, the framework of two samples synthesized from nonaqueous media might contain multiple environments of Si coordination, including species with silanol groups, as compared with that of the S0 sample synthesized from the aqueous medium.

NH_3-IR measurements were utilized to differentiate the acidic strength of the samples. NH_3-IR spectra of all the samples at different desorption temperatures are presented in figure 5 in the range of 1800 cm^{-1} to

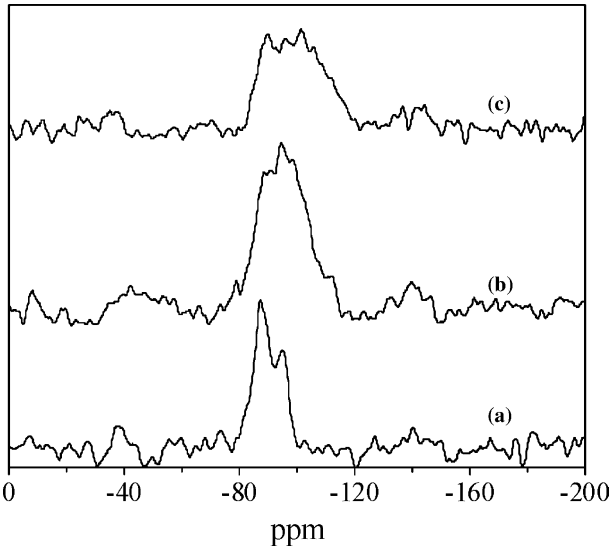

Figure 4. $^1H \rightarrow {}^{29}Si$ CP/MAS NMR of the SAPO-11 samples [(a) S0 (TEOS, IPA, H_2O); (b) S3(TEOS, IPA, EG); (c) S4(TEOS, PB, EG)].

1250 cm^{-1}. The bands at 1457 cm^{-1} and 1619 cm^{-1} can be ascribed to the adsorption of NH_3 molecules on the Bronsted acid sites and Lewis acid sites, respectively [4]. With an increase of the desorption temperature from 100 °C to 200 °C, the intensities of both the bands at 1619 and 1456 cm^{-1} for all the samples decreased. When the desorption temperature was increased to 300 °C, the band at 1456 cm^{-1} for the S0 sample synthesized from the aqueous medium disappeared completely, while 20% and 10% of the band intensities for the S3 and S4 samples, respectively, were left behind. This result clearly implied that the Bronsted acid strengths of the S3 and S4 samples synthesized from nonaqueous media are stronger that that of the S0 samples synthesized from the aqueous system, and S3 had the highest acidity among these samples. According to the literature [references 13,17,18 and 21], Bronsted acidic sites at the border of Si domains usually have higher acidic strength than acidic sites in SAPO domains, which are formed by a simple SM2 substitution. Combining the XRF and the ^{29}Si CP MAS NMR results, it can be proposed that the strong acidic sites of the S3 and S4 samples (corresponding to NH_3 desorption temperature of higher than 300 °C) synthesized from nonaqueous media might result from the borders of the Si domains, which can occur in high Si content SAPO-11 molecular sieves.

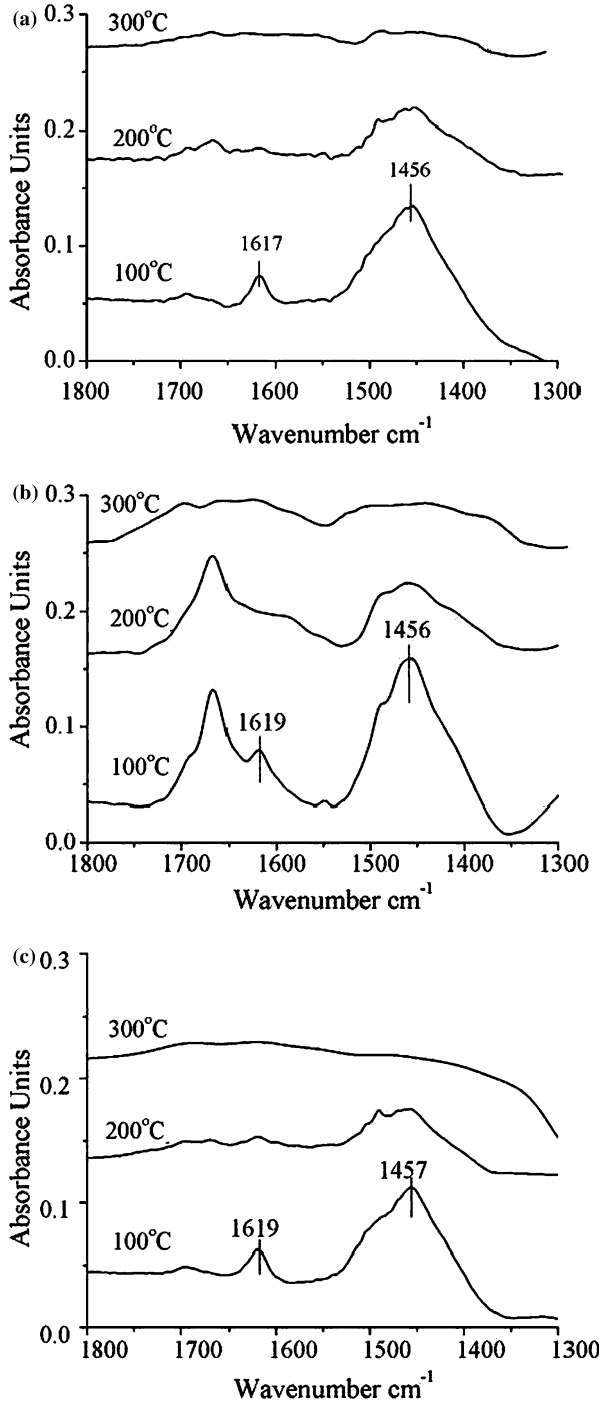

Figure 5. NH_3-IR spectra of the SAPO-11 samples synthesized [(a) S0 (TEOS, IPA, H_2O); (b) S3(TEOS, IPA, EG); (c) S4(TEOS, PB, EG)].

3.4. Hydroisomerization of n-Dodecane

Hydroisomerization of *n*-dodecane was carried out to evaluate the catalytic properties of all the catalysts, which were supported on the synthesized SAPO-11 molecular sieves. The conversion of *n*-dodecane as a function of the reaction temperature is presented in figure 6. For all the catalysts, the conversion of *n*-dodecane is a unique function of reaction temperature. It was observed that the hydroisomeization activities of all the catalysts follow the order of Pt/S3 > Pt/S5 > Pt/S2 > Pt/S4 > Pt/S1 > Pt/S0. The Pt/SAPO-11 catalysts on supports synthesized from nonaqueous media exhibited higher catalytic activities than the Pt/S0 catalyst synthesized from the aqueous medium. Of all the catalysts synthesized from the nonaqueous media, the Pt/S3 and Pt/S5 catalysts, with TEOS and IPA as the Si and Al sources, respectively, exhibited higher catalytic activities. Especially, the Pt/S3 catalyst supported on the

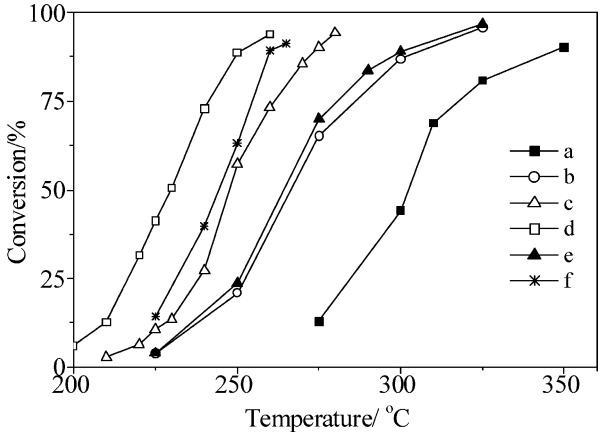

Figure 6. Conversion of n-C_{12} as a function of temperature over the Pt/SAPO-11 catalysts at WHSV = 1.0 h^{-1} and H_2/n-C_{12}(mol) = 15 [(a) Pt/S0 (TEOS, IPA, H_2O); (b) Pt/S1(Si colloidal gel, IPA,EG); (c) Pt/S2 (Fumed silica, IPA, EG); (d) Pt/S3 (TEOS, IPA, EG); (e) Pt/S4(TEOS, PB, EG); (f) Pt/S5(TEOS, IPA, glycerol)].

molecular sieve synthesized from the EG medium exhibited the highest catalytic activity. Over this catalyst, 88.7% n-C_{12} conversion was achieved at a rather low temperature of 250 °C (shown in table 3).

Hydroisomerization selectivity as a function of conversion of n-C_{12} is shown in figure 7. With an increase in n-C_{12} conversion, the hydroisomerization selectivity decreased slightly, which can be explained as due to the consumption of the isomeric products in consecutive hydrocracking. The Pt/SAPO-11 catalysts, having supports synthesized from nonaqueous media, showed higher hydroisomerization selectivity, as compared with that of the Pt/S0 catalyst with its support synthesized from the aqueous medium. Even at high n-dodecane conversions (>80%), these catalysts with supports synthesized from non-aqueous media exhibited good hydroisomerization selectivities (about 90%). As has been known, hydrocracking of alkanes is an endothermal reaction, and is thus thermodynamically favored at high temperatures. On the contrary, as the hydroisomerization reaction is a slightly exothermic reaction, it is favored at low temperatures. As has been mentioned above, owing to their higher activities, at equal conversion of n-dodecane, the reaction temperatures needed for these catalysts were much lower than that for the Pt/S0 with the support synthesized from the aqueous medium. It is because at lower reaction temperatures, the hydrocracking reaction is suppressed to some extent, so that higher selectivities to isomeric products over these catalysts can be achieved.

Table 3 shows the results of hydroisomerization of n-dodecane over the catalysts at about 90% n-C_{12} conversion. For all the catalysts, mono-branched isomers were predominant in the isomeric products. This preferential formation of the mono-branched isomers over the Pt/SAPO-11, SAPO-31 and SAPO-41 catalysts was attributed to the restricted-transition selectivities [13]. In the narrow channels of these 10-membered ring molecular sieves, the constraint imposed by the limited space in the pores has a significant influence on the formation of carbenium intermediates. The mono-branched carbeniums are smaller in size than those of multi-branched carbeniums, and thus are highly favored. Moreover, it was found that the catalysts with supports synthesized from the nonaqueous media gave higher hydroisomerization yields than the Pt/S0 catalyst with the support synthesized from the aqueous medium. This can be attributed to the high hydrosiomerization selectivities of those catalysts having supports synthesized from the nonaqueous media.

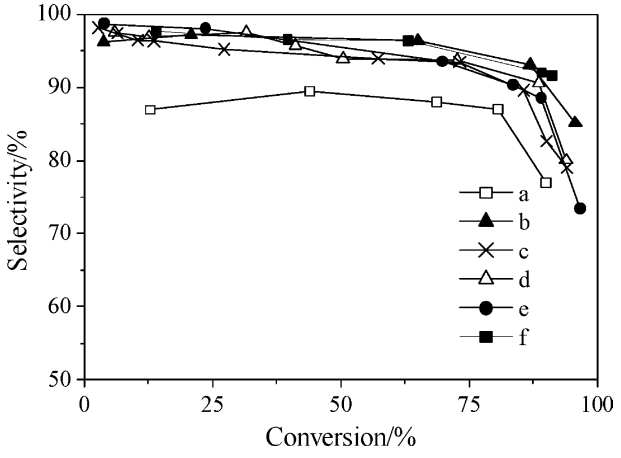

Figure 7. Hydroisomerization selectivity as a function of n-C_{12} conversion over the Pt/SAPO-11 catalysts at WHSV = 1.0 h^{-1} and H_2/n-C_{12}(mol) = 15 [(a) Pt/S0 (TEOS, IPA, H_2O); (b) Pt/S1(Si colloidal gel, IPA,EG); (c) Pt/S2 (Fumed silica, IPA, EG); (d) Pt/S3 (TEOS, IPA, EG); (e) Pt/S4(TEOS, PB, EG); (f) Pt/S5(TEOS, IPA, glycerol)].

The higher catalytic activities of the Pt/S3 and Pt/S5 catalysts, the supports of which were synthesized from EG and glycerol media, respectively, and with monomeric Si and Al resources (TEOS and IPA, respectively), can be attributed to their higher acidities. For bi-functional catalysts, acidity is one of the key factors in determining the catalytic activities [15], and this fact is verified by our catalysts with supports synthesized from nonaqueous media and having high acidities, as they all exhibited high catalytic activities for hydroisomerization of n-C_{12}. Moreover, This might also be due to their larger external surface areas and smaller crystallite sizes, as compared with the other catalysts. Due to their larger external surface areas, more micropores were developed in these two catalysts with supports synthesized from the nonaqueous media, thus improving their catalytic activities. Furthermore, it is well known that over shape selective molecular sieve catalysts, such as ZSM-5, ZSM-22 and SAPO-11, the effect of diffusion limitation on the reaction rate is very pronounced because of the sizes of the reactants, the intermediates and the products are quite close to the micropore sizes of these molecular sieves [4]. Generally speaking, a reduction in the crystallite size of the molecular sieves can significantly decrease the diffusion limitation, which is beneficial in enhancing the catalytic activities of the catalysts. Therefore, due to its relatively high acidity, large external surface area and small crystallite size, of all the catalysts studied in this work, the Pt/S3 catalyst exhibited the highest catalytic activity for hydroisomerization of n-C_{12}.

4. Conclusions

In nonaqueous media, monomeric Si (tetraethoxysilane) as the silicon source favored more Si incorporation into the framework of the SAPO-11 molecular sieves, as compared with the polymeric Si sources (fumed silica or Si colloidal gel) . The reaction results showed that the Pt/SAPO-11 catalysts, with the support synthesized from ethylene glycol or glycerol media and with monomeric Si and Al sources (tetraethoxysilane and aluminum isopropoxide, respectively) exhibited higher catalytic

Table 3
Results of *n*-Dodecane hydroisomerization over Pt/SAPO-11 catalysts (WHSV = 1.0 h^{-1}, $H_2/n\text{-}C_{12}$(mol) = 15)

Catalyst	Pt/S0	Pt/S1	Pt/S2	Pt/S3	Pt/S4	Pt/S5
Temperature/°C	350	300	270	250	300	260
Conversion/%	90.1	87.0	85.7	88.7	89.1	89.2
Selectivity%	77.0	93.0	89.6	90.5	88.5	92.0
Iso-Yield%	69.4	80.9	76.8	80.3	78.8	82.1
[a]Mono-yield/%	53.4	51.7	53.9	51.3	54.8	58.3
[b]Multi-yield/%	16.0	29.2	22.8	29.0	24.0	23.8

[a]mono-branched *i*-C_{12} yield; [b]multi-branched *i*-C_{12} yield.

activities than the catalysts with polymeric Si source or Al source (pseudo-boehmite) . This was due to their larger external surface areas and higher acidities. Especially, the catalyst with its support synthesized in an ethylene glycol medium possessed the highest catalytic activity.

Acknowledgments

The authors are grateful to Mrs. GUAN Jing and Mrs. LIU Xiumei for performing solid NMR determinations, and to Prof. HAN Xiuwen for helpful discussions on the NMR spectra.

References

[1] Miller S.I., US Patent 5,135,638 (1992).
[2] S.J. Miller, Stud. Surf. Sci. Catal. 84 (1994) 2319.
[3] P. Mériaudeau, V.A. Tuan, V.T. Nghiem, S.Y. Lai, L.N. Hung and C. Naccache, J. Catal. 169 (1997) 55.
[4] J.M. Campelo, F. Lafont and J.M. Marinas, J. Chem. Soc. Faraday Trans. 91 (1995) 1551.
[5] J.A. Martens, R. Parton, L. Uytterhoeven, P.A. Jacobs and G.F. Froment, Appl. Catal. 76 (1991) 95.
[6] F. Alvarez, F.R. Ribeiro, G. Perot, C. Thomazeau and M. Guisnety, J. Catal. 162 (1996) 179.
[7] L.B. Galperin, Appl. Catal. A 209 (2001) 257.
[8] K.C. Park and S.K. Ihm, Appl. Catal. A 203 (2000) 201.
[9] M.C. Claude, G. Vanbutsele and J.A. Martens, J. Catal. 203 (2001) 213.
[10] S. Ernst, R. Kumar and J. Weitkamp, Catal. Today 3 (1988) 1.
[11] J.M. Campelo, F. Lafont and J.M. Marinas, Appl. Catal. A 170 (1998) 139.
[12] A.K. Sinha, S. Sivasanker and P. Ratnasamy, Ind. Eng. Chem. Res. 37 (1998) 2208.
[13] P. Mériaudeau, Vu. A. Tuan, F. Lefebvre, Vu. T. Nghiem and C. Naccache, Micropor. Mesopor. Mater. 22 (1998) 435.
[14] M.L. Goonradt and W.E. Garwood, Ind. Eng. Chem. Proc. Res Dev. 3 (1964) 38.
[15] M. Höchtl, A. Jentys and H. Vinek, J. Catal. 190 (2000) 419.
[16] E.M. Flanigen, R.L. Patton and S.T. Wilson, Stud. Surf. Sci. Catal. 37 (1988) 13.
[17] M. Martens, J.A. Martens, P.J. Grobet and P.A. Jacobs, in: *Guidelines for Mastering the Properties of Molecular Sieves*, eds. D. Barthomeuf, E.G. Derouane and W. Holderich (Plenum Press, New York, 1990), Chap. 1, p. 1.
[18] M.M. Makarova, A. Ojo, K. Al-Ghefaili and J. Dwyer, in: Proceedings of 9th International Zeolite Conference, Montreal, eds. R. von Ballmoos, J.B. Higgins and M.M.Treacy (Butterworth-Heinemann, Boston, 1992), vol. 2, p. 259.
[19] L. Marchese, J. Chen, P.A. Wright and J.M. Thomas, J. Phys. Chem. 97 (1993) 8109.
[20] M. Alfonzo, J. Goldwasser, C.M. López, F.J. Machado M. Matjushin, B. Méndez and M.M. Ramírez de Agudelo, J. Mol. Catal. A 98 (1995) 35.
[21] J.A. Martens, P.J. Grobet and P.A. Jacobs, J. Catal. 126 (1990) 299.
[22] Q. Huo and R. Xu, J. Chem. Soc., Chem. Commun. 783 (1990).
[23] R. Xu, Q. Huo and W. Pang, Proc. 9th Inter. Zeol. Confer., Montreal, eds. R.V. Ballmoos et al. 1992, p. 271.
[24] S. Seelan and A.K. Sinha, J. Mol. Catal. A 215 (2004) 149.
[25] A.K. Sinha and S. Seelan, Appl. Catal. A 270 (2004) 245.
[26] B. Parlitz, E. Schreier, H. Zubova, R. Eckelt, E. Lieske, G. Lischke and R. Fricke, J. Catal. 155 (1995) 1.
[27] M. Alfonzo, J. Goldwasser, C.M. López, F.J. Machado M. Matjushin, B. Méndez and M.M. Ramírezde Agudelo, J. Mol. Catal. A 98 (1995) 35.
[28] D. Barthomeuf, Zeolites 14 (1994) 394.